

MIT Open Access Articles

Role of Disorder and Anharmonicity in the Thermal Conductivity of Silicon-Germanium Alloys: A First-Principles Study

The MIT Faculty has made this article openly available. **Please share** how this access benefits you. Your story matters.

Citation: Garg, Jivtesh et al. "Role of Disorder and Anharmonicity in the Thermal Conductivity of Silicon-Germanium Alloys: A First-Principles Study." Phys. Rev. Lett. 106, 045901 (2011). © 2011 American Physical Society.

As Published: <http://dx.doi.org/10.1103/PhysRevLett.106.045901>

Publisher: American Physical Society

Persistent URL: <http://hdl.handle.net/1721.1/63802>

Version: Final published version: final published article, as it appeared in a journal, conference proceedings, or other formally published context

Terms of Use: Article is made available in accordance with the publisher's policy and may be subject to US copyright law. Please refer to the publisher's site for terms of use.



Role of Disorder and Anharmonicity in the Thermal Conductivity of Silicon-Germanium Alloys: A First-Principles Study

Jivtesh Garg,^{1,5} Nicola Bonini,^{2,3} Boris Kozinsky,⁴ and Nicola Marzari^{2,3,5}

¹*Department of Mechanical Engineering, Massachusetts Institute of Technology, Cambridge, Massachusetts 02139, USA*

²*Department of Materials Science and Engineering, Massachusetts Institute of Technology, Cambridge, Massachusetts 02139, USA*

³*Department of Materials, University of Oxford, Oxford OX1 3PH, United Kingdom*

⁴*Robert Bosch LLC, Research and Technology Center, Cambridge, Massachusetts 02139, USA*

⁵*Institute for Soldier Nanotechnologies, Massachusetts Institute of Technology, Cambridge, Massachusetts 02139, USA*

(Received 10 July 2010; revised manuscript received 12 September 2010; published 24 January 2011)

The thermal conductivity of disordered silicon-germanium alloys is computed from density-functional perturbation theory and with relaxation times that include both harmonic and anharmonic scattering terms. We show that this approach yields an excellent agreement at all compositions with experimental results and provides clear design rules for the engineering of nanostructured thermoelectrics. For $\text{Si}_x\text{Ge}_{1-x}$, more than 50% of the heat is carried at room temperature by phonons of mean free path greater than $1\ \mu\text{m}$, and an addition of as little as 12% Ge is sufficient to reduce the thermal conductivity to the minimum value achievable through alloying. Intriguingly, mass disorder is found to increase the anharmonic scattering of phonons through a modification of their vibration eigenmodes, resulting in an increase of 15% in thermal resistivity.

DOI: 10.1103/PhysRevLett.106.045901

PACS numbers: 66.70.-f, 63.20.dk, 63.20.kg, 63.50.Gh

The energy conversion efficiency of a thermoelectric device is often characterized by the dimensionless figure of merit $ZT = S^2\sigma T/k$, where S , σ , k , and T are the Seebeck coefficient, electrical conductivity, thermal conductivity, and temperature, respectively. One of the most promising avenues to increase ZT beyond ~ 1 has been to reduce thermal conductivity through enhanced phonon scattering following alloying, surface roughening, or nanostructuring [1–3]. While mass disorder plays a key role in lowering thermal conductivity in important thermoelectric materials such as half-Heusler alloys [4] and silicon-germanium alloys, an attempt to predict the magnitude of this effect in SiGe alloys through nonequilibrium molecular dynamics [5] simulations using the Stillinger-Weber potential [6] resulted in large discrepancies with measured values. Furthermore, it is not known what effect, if any, mass disorder has on anharmonic scattering of phonons. An understanding of this effect could provide avenues for optimizing it to increase ZT by further lowering the thermal conductivity. In predicting thermal conductivity, empirical potentials are often used, but these do not necessarily yield the correct thermal conductivity [7] and are often untested in their anharmonic behavior around equilibrium. On the other hand, Broido *et al.* [8] used the harmonic and anharmonic force constants of Si^{28} and Ge^{70} derived from first principles through the density-functional perturbation theory [9–11], to compute thermal conductivities, with excellent agreement between calculated and measured results.

Abeles [12] first introduced the idea of computing the thermal conductivity of SiGe alloys by replacing the disordered crystal with an ordered one and treating both

disorder and anharmonicity as perturbations. In this phenomenological model the net scattering rate of a phonon mode is computed as the sum of the scattering due to mass disorder and anharmonicity. The former is taken to be $\tau^{-1} = \omega^4 V_0 g / (4\pi v^3)$, in analogy with the result of Klemens [13] for point-defect scattering [V_0 is the volume per unit atom, v is the branch-averaged sound velocity, $g = \sum_i f_i (1 - m_i/\bar{m})^2$ is a measure of the mass disorder, f_i and m_i are the concentration and the atomic mass of species i , respectively, and \bar{m} is the average mass for the given composition]. For the latter, the low-frequency limit of normal ($B_1\omega^2$) and umklapp ($B_2\omega^2$) processes is used to estimate anharmonic scattering. The use of these fitting parameters provides good agreement with experiments but also limits the predictive ability of these models.

In this Letter, we present a fully first-principles approach to compute the thermal conductivity of SiGe alloys with all parameters derived from the density-functional perturbation theory. Following Ref. [12] we calculate at any composition the phonon modes of the virtual crystal (which has a 2-atom diamond unit cell and lattice parameter, mass, and force constants appropriate to that particular composition) and derive from those the frequencies, group velocities, and populations that enter into the calculation of thermal conductivity. The force constants and lattice parameter are interpolated quadratically at any composition using the end points (pure Si and Ge) and the virtual crystal at $x = 0.5$, where the external atomic potential at every lattice site is given by the average of the Si and Ge pseudopotentials [14,15]. Finally, we adopt the single-mode relaxation time approximation [16] as an approximate solution of the Boltzmann transport equation [17,18]; the thermal

conductivity $k_{\alpha\beta}$ (defined by the heat current in the α th direction for a temperature gradient along the β direction) is then given by

$$k_{\alpha\beta} = \frac{\hbar^2}{N\Omega k_B T^2} \sum_{\lambda} c_{\alpha\lambda} c_{\beta\lambda} \omega_{\lambda}^2 n_{\lambda} (n_{\lambda} + 1) \tau_{\lambda}, \quad (1)$$

where α and β are the Cartesian directions, c , ω , n , and τ are the phonon group velocities, frequencies, equilibrium populations, and relaxation times, respectively, λ represents the vibrational mode (\mathbf{q} , j) (\mathbf{q} is the wave vector and j the phonon branch), and T , Ω , and N are the temperature, cell volume, and size of the \mathbf{q} -point mesh, respectively. The scattering rate $1/\tau_{\lambda}$ of a phonon mode λ is taken to be the sum of a term describing harmonic scattering due to mass disorder ($1/\tau_{\lambda a}$) and a term describing anharmonic scattering ($1/\tau_{\lambda b}$) as in Matthiessen's rule.

The harmonic scattering rates due to mass disorder are calculated by using perturbation theory [19]:

$$\frac{1}{\tau_{\lambda a}} = \frac{\pi}{2} g \omega_{\lambda}^2 D(\omega_{\lambda}), \quad (2)$$

where g (defined before) takes into account the magnitude of mass disorder and $D(\omega)$ is the phonon density of states (normalized to unity) of the virtual crystal. Though the expression for harmonic scattering [Eq. (2)] is valid for small mass disorder, its use leads to good agreement with experimentally measured phonon linewidths, even in the case of the $\text{Ni}_{0.55}\text{Pd}_{0.45}$ alloy, where the atomic species are chemically similar but mass disorder is large ($m_{\text{Pd}}/m_{\text{Ni}} = 1.812$) [20].

The anharmonic scattering rates are computed by using the lowest-order three-phonon scattering processes in the single-mode relaxation time approximation via [9,21]

$$\frac{1}{\tau_{\lambda b}} = \pi \sum_{q', j', q'', j''} |V_3(j, -\mathbf{q}; j', \mathbf{q}'; j'', \mathbf{q}'')|^2 \times [(1 + n_{j'q'} + n_{j''q''})\delta(\omega_{j'q'} + \omega_{j''q''} - \omega_{j,-q}) + 2(n_{j''q''} - n_{j'q'})\delta(\omega_{j'q'} - \omega_{j''q''} - \omega_{j,-q})], \quad (3)$$

where $V_3(j, -\mathbf{q}; j', \mathbf{q}'; j'', \mathbf{q}'')$ are the three-phonon coupling matrix elements [21]. These anharmonic scattering rates for any composition are computed first by using the phonon modes of the virtual crystal corresponding to that composition; later we will also incorporate the effect of disorder by performing explicit calculations on supercells with random distributions of Si and Ge masses for the relevant composition. The 2nd- and 3rd-order interatomic force constants are obtained on a $10 \times 10 \times 10$ and $3 \times 3 \times 3$ supercell, respectively; for all density-functional perturbation theory calculations a $8 \times 8 \times 8$ Monkhorst-Pack [22] mesh is used to sample electronic states in the Brillouin zone, and an energy cutoff of 20 Ry is used for the plane-wave expansion. We carefully tested convergence of all measured quantities with respect to these parameters. First-principles calculations within density-functional theory are carried out by using the PWSCF and

PHONON codes of the QUANTUM-ESPRESSO distribution [23] with norm-conserving pseudopotentials based on the approach of von Barth and Car [24].

The approach outlined above yields an excellent agreement between the computed and measured values at 300 K [12,25] for the alloy thermal conductivity at all compositions (Fig. 1). Notably, the thermal conductivity is found to drop sharply after only a small amount of alloying. This is due to the strong harmonic scattering of phonons even in the dilute alloy limit. Our approach predicts that in the composition range $0.2 < x < 0.8$ the alloy thermal conductivity becomes nearly independent of composition, in excellent qualitative and quantitative agreement with experiments.

This low thermal conductivity in $\text{Si}_x\text{Ge}_{1-x}$ with respect to pure Si or pure Ge is better understood from the analysis of the relative contribution of the different scattering mechanisms. As shown in Fig. 2(a) for $\text{Si}_{0.5}\text{Ge}_{0.5}$, thermal conductivity even at temperatures as high as 500 K is dominated by phonon modes below 1 THz (at 100, 300, and 500 K, respectively, 82%, 65%, and 58% of the heat is conducted by phonons of frequency less than 1 THz, while 13%, 23%, and 27% is conducted by phonons between 1 and 2 THz; optical frequencies for Si and Ge are 15.67 and 9.27 THz, respectively, at the zone center). In pure silicon, on the other hand, phonon modes up to 6 THz contribute in similar measures to thermal conductivity [Fig. 2(a)]; harmonic scattering [Fig. 2(b)] completely annihilates the heat-carrying ability of these higher frequency modes leading to the observed sudden drop in conductivity.

While disagreement with measured resistivity value [26] is less than 10% at 300 K for $\text{Si}_{0.3}\text{Ge}_{0.7}$, it becomes larger at higher temperatures [open squares in Fig. 3(a)]. Though the effect of four-phonon processes has been estimated to be small [27], we should note that up to now scattering rates were computed by using the phonon modes of the virtual crystal, without taking into account the effect of a random

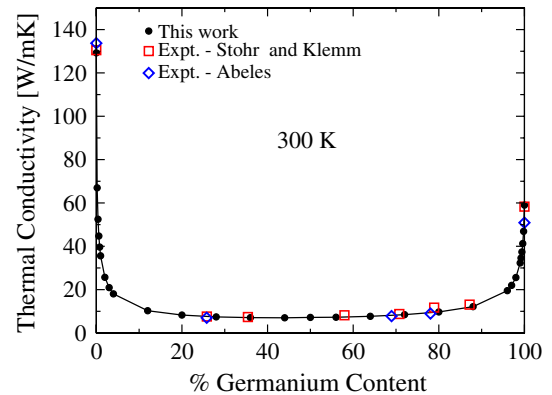


FIG. 1 (color online). Composition dependence of the thermal conductivity in $\text{Si}_x\text{Ge}_{1-x}$ at 300 K. Solid black circles show our predicted thermal conductivities, to be compared with the experimental values of Stohr and Klemm (Ref. [25]) and Abeles (Ref. [12]) (red open squares and blue open diamonds, respectively).

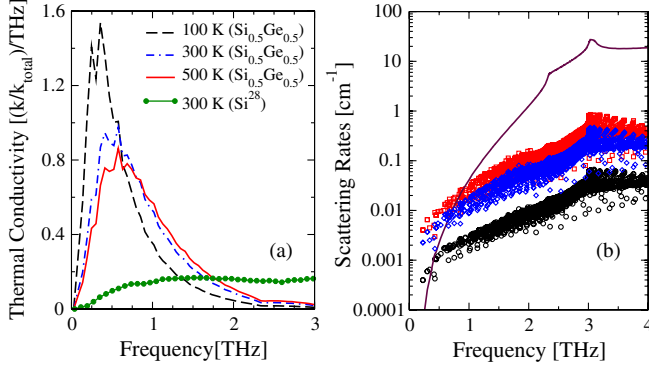


FIG. 2 (color online). (a) Frequency dependence of the thermal conductivity (normalized with respect to total thermal conductivity) for $\text{Si}_{0.5}\text{Ge}_{0.5}$ and pure silicon. (b) Scattering rates (full width at half maximum) due to harmonic scattering (solid line) and anharmonic scattering (open symbols) in $\text{Si}_{0.5}\text{Ge}_{0.5}$. Open circles, diamonds, and squares are the anharmonic scattering rates at 100, 300, and 500 K, respectively. Below 0.7 THz, the mass-disorder scattering rate agrees well with Klemens' result for point-defect scattering: $\tau_{\lambda\alpha}^{-1} = 4.43 \times 10^{-42} \times \omega_{\lambda}^4 \text{ sec}^{-1}$, where ω is in rad/sec.

distribution of masses. To incorporate this effect, we compute the scattering rates by using large supercells with explicit random distribution of Si and Ge masses in the relevant compositions. Figure 4(a) shows that for $\text{Si}_{0.3}\text{Ge}_{0.7}$ the anharmonic phonon relaxation times computed by using a $4 \times 4 \times 4$ supercell (dashed red line) are lower by a factor of ~ 2.0 at the smallest frequencies studied—compared to those obtained by using the virtual crystal (solid black line)—with the difference diminishing as the frequency is increased. Using these lower anharmonic lifetimes, and continuing to use the other parameters obtained with the virtual crystal, we find that a good agreement with measured resistivity values is obtained even at higher temperatures [see Fig. 3(a), open diamond]. On the other hand, the effect of using real masses is negligible for

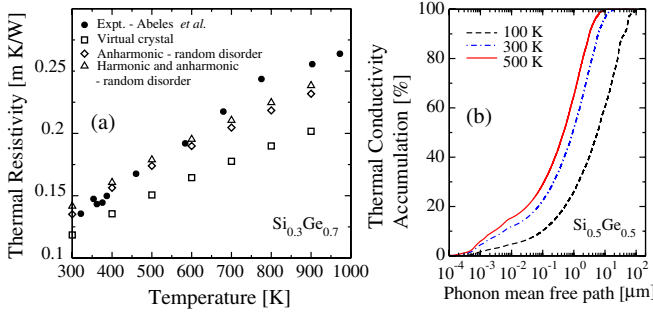


FIG. 3 (color online). (a) Temperature dependence of the thermal resistivity; measured values are from Ref. [26]. The open squares and the open diamonds are the computed values obtained by using anharmonic relaxation times of the virtual crystal and the supercell (where disorder is simulated through explicit random distribution of Si and Ge masses appropriate to $\text{Si}_{0.3}\text{Ge}_{0.7}$), respectively. (b) Accumulation of the thermal conductivity for $\text{Si}_{0.5}\text{Ge}_{0.5}$ as a function of the phonon mean free path.

harmonic scattering in the low-frequency region, due to the negligible changes in phonon density of states at low frequencies [Fig. 4(b)], resulting in minimal changes for the thermal resistivity [open triangles in Fig. 3(a)].

Mass disorder thus lowers thermal conductivity through harmonic scattering in the high-frequency region and by increasing anharmonic scattering at low frequencies. To understand this latter effect, we perform anharmonic scattering calculations on a $2 \times 2 \times 2$ supercell, using 2nd- and 3rd-order force constants for the composition $\text{Si}_{0.3}\text{Ge}_{0.7}$. We compute the values of the three-phonon anharmonic coupling matrix elements $|V_3(j, -\mathbf{q}; j', \mathbf{q}'; j'', \mathbf{q}'')|^2$ involved in the scattering of a low-frequency phonon mode ($\mathbf{q}j$), when the mode ($\mathbf{q}'j'$) is varied over the entire Brillouin zone. The $|V_3|^2$ values are computed first for the case where all the atoms have an average mass corresponding to $\text{Si}_{0.3}\text{Ge}_{0.7}$ and second with real Si and Ge masses randomly distributed according to the above composition. We find that in the first case a large fraction of channels have negligibly small $|V_3|^2$ [Fig. 5(a)], while in the second case the number of channels with large $|V_3|^2$ increases significantly [Fig. 5(b)], causing the overall anharmonic scattering rate to increase by almost a factor of 2. To explain this increase, we notice that $V_3(j, \mathbf{q}; j', \mathbf{q}'; j'', \mathbf{q}'') \sim \sum_{\kappa\kappa'\kappa''} \Phi_{\alpha\alpha'\alpha''}^{\kappa\kappa'\kappa''}(\mathbf{q}, \mathbf{q}', \mathbf{q}'') \tilde{e}_{\alpha}^{\kappa}(j\mathbf{q}) \tilde{e}_{\alpha'}^{\kappa'}(j'\mathbf{q}') \tilde{e}_{\alpha''}^{\kappa''}(j''\mathbf{q}'')$, where κ denotes the atoms in the supercell, α is the Cartesian direction, Φ is the Fourier transformed anharmonic force constants, $\tilde{e}_{\alpha}^{\kappa}(j\mathbf{q}) \equiv e_{\alpha}^{\kappa}(j\mathbf{q})/\sqrt{M_{\kappa}}$, M is the atomic mass, and e 's are the vibration eigenvectors. Typically, it is found that largest values of Φ involve the same atom and vibration along different Cartesian directions, while other terms are orders of magnitude smaller. Therefore $V_3 \sim \chi S$, where $S = \sum_{\alpha \neq \alpha' \neq \alpha''} \tilde{e}_{\alpha}^{\kappa}(j\mathbf{q}) \tilde{e}_{\alpha'}^{\kappa'}(j'\mathbf{q}') \tilde{e}_{\alpha''}^{\kappa''}(j''\mathbf{q}'')$. This is confirmed by the strong correlation between $|S|^2$ [Figs. 5(c) and 5(d)] and $|V_3|^2$ ($|S|^2$ can be thought of as an “eigenvector overlap”). Since the same anharmonic force constants are used for both cases of average or random masses, the difference in V_3 originates from the vibration eigenmodes. The small values of $|S|^2$ [Fig. 5(c)] in the average case indicate a

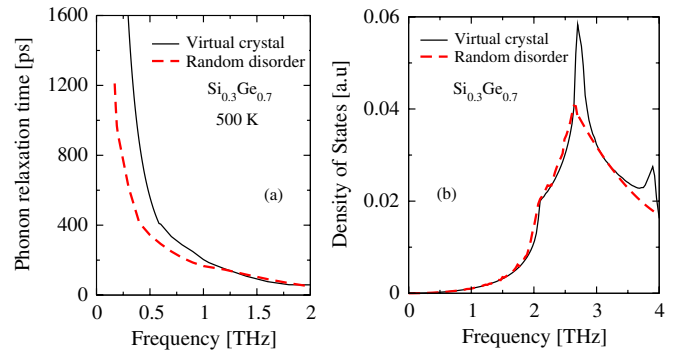


FIG. 4 (color online). (a) Anharmonic relaxation times and (b) phonon density of states—computed by using the virtual crystal (solid black line) and $4 \times 4 \times 4$ supercell (dashed red line).

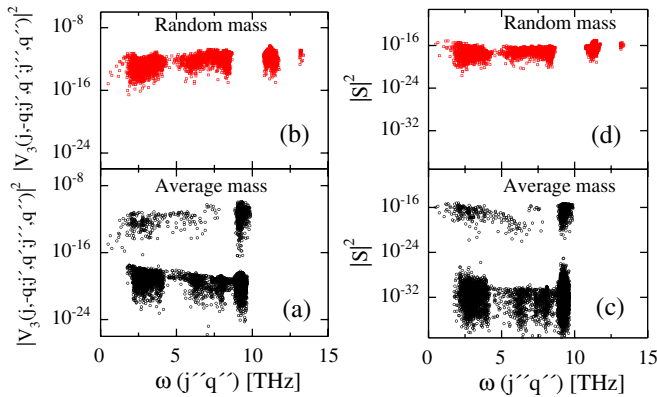


FIG. 5 (color online). Three-phonon coupling matrix elements ($|V_3|^2$) and eigenvector overlap ($|S|^2$) computed for $\text{Si}_{0.3}\text{Ge}_{0.7}$ on a $2 \times 2 \times 2$ supercell by using (a),(c) average mass and (b),(d) a random distribution of masses.

cancellation of terms involved in the summation for S —due to an even distribution of vibration amplitudes over all atoms in the system—while a random distribution perturbs this even distribution, preventing such cancellation.

The predictive power of first-principles calculations allows us to lay out design rules for low thermal conductivity materials, of central importance for applications in thermoelectrics. For example, we show that at 300 K [Fig. 3(b)] most of the heat is conducted by phonons with mean free paths around $1 \mu\text{m}$ (60% between 0.2 and $3 \mu\text{m}$). Additional scattering mechanisms introduced by the presence of grain boundaries or nanoparticles distributed around these optimal values can thus reduce the phonon mean free path and the thermal conductivity below the bulk alloy value. Indeed, Rowe, Shukla, and Savvides [28] showed that introduction of grain boundaries can reduce the thermal conductivity of SiGe alloys by as much as $\sim 28\%$. Similarly, from Fig. 1, it can be seen that addition of only about 12% Ge to Si is sufficient to lower the thermal conductivity to the minimum value achievable in this binary system, of central importance to develop low-cost thermoelectric devices.

In conclusion, we have presented an approach to compute thermal conductivity of alloys at any composition, in which all the ingredients—vibrational modes and harmonic and anharmonic scattering rates—are computed from first principles. This approach accurately reproduces the available experimental results for alloy conductivity and predicts the minimum level of alloying sufficient to achieve the maximum reduction in conductivity in alloys. Furthermore, a microscopic characterization of the relative contribution of the different vibrational modes in terms of their mean free paths provides practical guidelines for nanostructuring to reduce the thermal conductivity below the bulk alloy limit. Finally and most interestingly, mass

disorder is found to result in an increased anharmonic scattering of phonons through a modification of their vibration eigenmodes.

We thank David Broido, Giulia Galli, Gyaneshwar P. Srivastava, Alistair Ward, and Davide Donadio for valuable discussions and suggestions. The work was supported by MIT's Institute for Soldier Nanotechnologies (ISN-ARO) under Grant No. W911NF-07-D-0004 (J. G. and N. B.) and Robert Bosch LLC (N. M.).

- [1] M. S. Dresselhaus *et al.*, *Adv. Mater.* **19**, 1043 (2007).
- [2] A. I. Hochbaum *et al.*, *Nature (London)* **451**, 163 (2008).
- [3] A. I. Boukai *et al.*, *Nature (London)* **451**, 168 (2008).
- [4] C. Uher *et al.*, *Phys. Rev. B* **59**, 8615 (1999).
- [5] A. Skye and P. K. Schelling, *J. Appl. Phys.* **103**, 113524 (2008).
- [6] F. H. Stillinger and T. A. Weber, *Phys. Rev. B* **31**, 5262 (1985).
- [7] D. A. Broido, A. Ward, and N. Mingo, *Phys. Rev. B* **72**, 014308 (2005).
- [8] D. A. Broido *et al.*, *Appl. Phys. Lett.* **91**, 231922 (2007).
- [9] A. Debernardi, S. Baroni, and E. Molinari, *Phys. Rev. Lett.* **75**, 1819 (1995).
- [10] S. Baroni, P. Giannozzi, and A. Testa, *Phys. Rev. Lett.* **58**, 1861 (1987).
- [11] X. Gonze, *Phys. Rev. A* **52**, 1086 (1995).
- [12] B. Abeles, *Phys. Rev.* **131**, 1906 (1963).
- [13] P. G. Klemens, *Proc. Phys. Soc. London Sect. A* **68**, 1113 (1955).
- [14] N. Marzari, S. de Gironcoli, and S. Baroni, *Phys. Rev. Lett.* **72**, 4001 (1994).
- [15] S. Baroni, S. deGironcoli, and P. Giannozzi, *Phys. Rev. Lett.* **65**, 84 (1990).
- [16] J. M. Ziman, *Electrons and Phonons* (Oxford University Press, London, 1960).
- [17] R. Peierls, *Ann. Phys. (Leipzig)* **3**, 1055 (1929).
- [18] R. Peierls, *Quantum Theory of Solids* (Clarendon Press, Oxford, 1955).
- [19] S. Tamura, *Phys. Rev. B* **27**, 858 (1983).
- [20] W. A. Kamitakahara and B. N. Brockhouse, *Phys. Rev. B* **10**, 1200 (1974).
- [21] G. Deinzer, G. Birner, and D. Strauch, *Phys. Rev. B* **67**, 144304 (2003).
- [22] H. J. Monkhorst and J. D. Pack, *Phys. Rev. B* **13**, 5188 (1976).
- [23] P. Giannozzi *et al.*, *J. Phys. Condens. Matter* **21**, 395502 (2009); <http://www.quantum-espresso.org>.
- [24] A. Dal Corso *et al.*, *Phys. Rev. B* **47**, 3588 (1993).
- [25] H. Stohr and W. Klemm, *Z. Anorg. Allg. Chem.* **241**, 304 (1954).
- [26] B. Abeles *et al.*, *Phys. Rev.* **125**, 44 (1962).
- [27] D. J. Ecsedy and P. G. Klemens, *Phys. Rev. B* **15**, 5957 (1977).
- [28] D. M. Rowe, V. S. Shukla, and N. Savvides, *Nature (London)* **290**, 765 (1981).